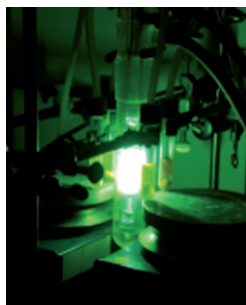


CONCEPTS

Bioinorganic Chemistry

G. Knör* 568–578

Artificial Enzyme Catalysis Controlled and Driven by Light




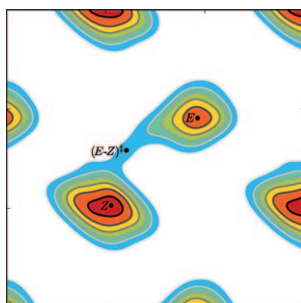
Bio-inspired chemistry! Photochemical key steps (see figure) provide a versatile tool for the remote control of chemical and biological processes. Many challenging reactions, which otherwise could hardly be achieved at all, are readily triggered and powered by photons. This Concept article explores the design principles and potential applications of biomimetic catalysis based on photoresponsive molecular systems.

COMMUNICATIONS

Azaallylic Anions

R. Declerck, B. De Sterck,
T. Verstraelen, G. Verniest,
S. Mangelinckx, J. Jacobs,
N. De Kimpe,* M. Waroquier,
V. Van Speybroeck* 580–584


 **Insight into the Solvation and Isomerization of 3-Halo-1-azaallylic Anions from Ab Initio Metadynamics Calculations and NMR Experiments**

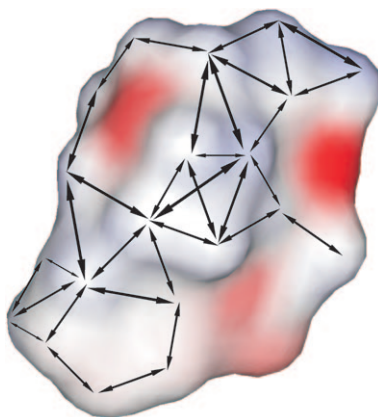


Long live the Z isomer! The solvation and isomerization properties of lithiated 3-chloro-1-azaallylic anions in tetrahydrofuran are revealed. Extensive and convincing evidence is obtained from state-of-the-art first-principle molecular dynamics and metadynamics simulations in an explicit periodic solvent model, together with detailed NMR experiments.

NMR Spectroscopy

C. M. Thiele,* K. Petzold,
J. Schleucher* 585–588


 **EASY ROESY: Reliable Cross-Peak Integration in Adiabatic Symmetrized ROESY**

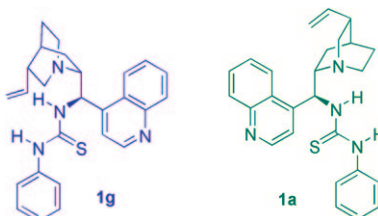


Estimates of intramolecular distances are essential for structure determination (see figure). For medium-sized molecules, ROESY NMR spectroscopy is the method of choice for obtaining distances. However, the integration of ROESY cross-peaks is problematic, owing to the offset dependence of the integrals and/or TOCSY artefacts. We here present EASY ROESY (Efficient Adiabatic SYmmetrized ROESY), which yields reliable intramolecular distances without a sample-specific setup.

Asymmetric Catalysis

F. Wang, X. Liu, X. Cui, Y. Xiong,
X. Zhou, X. Feng * 589–592

 **Asymmetric Hydrophosphonylation of α -Ketoesters Catalyzed by Cinchona-Derived Thiourea Organocatalysts**



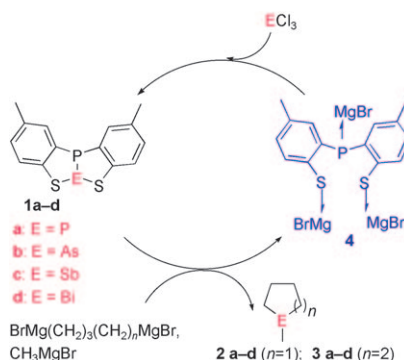
Naturally catalytic: The cinchonidine- and cinchonine-derived bifunctional thiourea organocatalysts **1a** and **1g** (see picture) have been applied in the asymmetric hydrophosphonylation of aromatic and heteroaromatic α -ketoesters for the first time, obtaining *S* and *R* products in high yields with good to excellent enantioselectivities (up to 91 % *ee*).



Ferrocene or ruthenocene? Computational (DFT) methods predicted a metal-dependent photochemistry for metallocenyl–chromium(0)–carbene

complexes (see scheme). These theoretical predictions are fully confirmed by the experimental results.

Maiden voyage: New arsenic-, antimony- and bismuth-donor reagents (**1b–d**) are used in a one-pot synthesis of cyclic arsanes, stibanes and bismutanes through a procedure in which the simultaneous formation of three C–As, C–Sb or C–Bi bonds is achieved. At the end of the reaction, the element-donor reagent can be easily re-formed “in situ” and recycled, as in a catalytic process.



Carbene Complexes

M. L. Lage, I. Fernández,*
M. J. Mancheño, M. Gómez-Gallego,
M. A. Sierra* 593–596

Metal-Tuned Photochemistry of Metallocene-Substituted Chromium(0)–Carbene Complexes

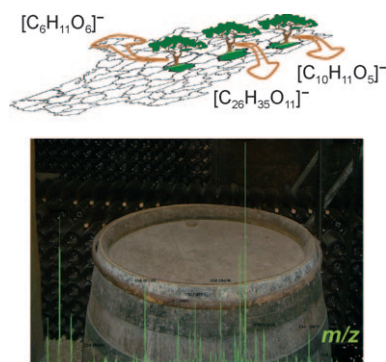
Heterocyclic Compounds

G. Baccolini,* C. Boga,*
M. Mazzacurati,
G. Micheletti 597–599

The First Flights of a Molecular Shuttle Transporting Elements: Easy One-pot Formation of Organic Cyclic Arsanes, Stibanes and Bismutanes

FULL PAPERS

From wood biochemistry to metabologeography: Non-targeted ultra-high-resolution Fourier transform ion cyclotron resonance mass spectroscopy (FTICR-MS) and NMR spectroscopy analyses show that broad chemical spaces particular to a given oak species in a given forest can manifest themselves in the composition of barrels and related barrel-aged wines (see graphic).



Multivariate Analysis

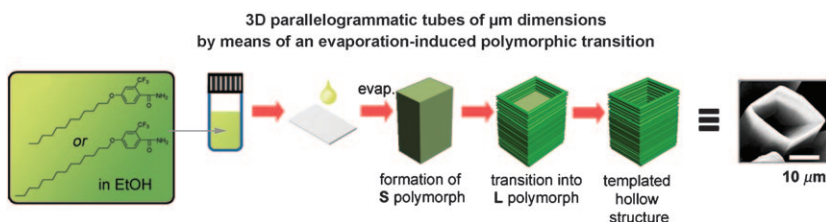
R. D. Gougeon,* M. Lucio,*
A. De Boel, M. Frommberger,
N. Hertkorn, D. Peyron, D. Chassagne,
F. Feuillat, P. Cayot, A. Voilley,
I. Gebefügi,
P. Schmitt-Kopplin* 600–611

Expressing Forest Origins in the Chemical Composition of Cooperage Oak Woods and Corresponding Wines by Using FTICR-MS

Porous Materials

M. Seo, J. H. Kim, G. Seo, C.-H. Shin,
S. Y. Kim* 612–622

Utilization of Evaporation during the Crystallization Process: Self-Templation of Organic Parallelogrammatic Pipes



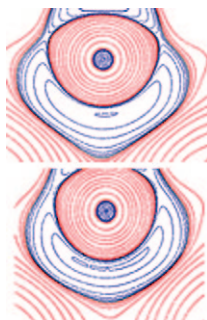
Hollow micropipes with parallelogrammatic shape can be obtained by simple evaporation of a solution of C₁₂ or C₁₄ alkoxy-2-trifluoromethylbenzamide on a substrate. A study on analogues with various alkyl chain lengths revealed that an evaporation-induced self-tem-

plated polymorphic transition, in which one polymorph acts as a template and the other as a negative replica, is responsible for the formation of hollow three-dimensional crystalline structures (see picture for schematic mechanism and SEM image of a pipe).

Metal–Metal Bonding

K. Götz, M. Kaupp,* H. Braunschweig,
D. Stalke 623–632

Comparative Analysis of Electron-Density and Electron-Localization Function for Dinuclear Manganese Complexes with Bridging Boron- and Carbon-Centered Ligands

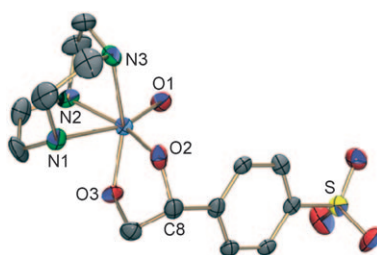


Borylene or substituted borane, metal–metal bond or none? For the borylene-bridged title complex and its analogues with bridging amino-borylene, methylene and vinylidene ligands, the second question gets a clear “no” from QTAIM and ELF analyses. But the first question depends, in a striking manner, on the computational method, due to an interesting bifurcation between two different bonding situations (top: B3LYP, bottom: BLYP plots).

Radiopharmacy

H. Braband, Y. Tooyama, T. Fox,
R. Alberto* 633–638

 **Syntheses of High-Valent *fac*-[^{99m}TcO₃]⁺ Complexes and [3+2] Cycloadditions with Alkenes in Water as a Direct Labelling Strategy**

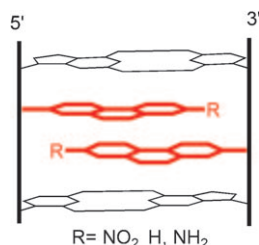


^{99m}Tc does it in water! The reaction of [^{99m}TcO₄][−] in water with phosphine-derivatised resins and triazacyclononane-based ligands gave the Tc^{VII} complexes [^{99m}TcO₃(N³)]⁺. In water, these complexes undergo [3+2] cycloadditions with alkenes to form Tc^V glycolato complexes (an example is shown here). Conjugation of alkenes to biomolecules thereby enables a direct labelling strategy, which is ligand- rather than metal-centred.

DNA Recognition

N. A. Grigorenko,
C. J. Leumann* 639–645

 **2-Phenanthrenyl–DNA: Synthesis, Pairing, and Fluorescence Properties**

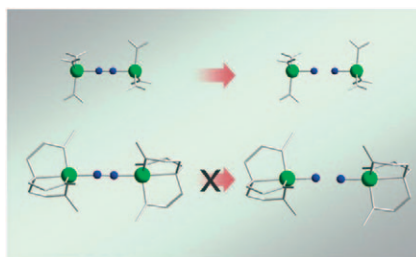


Bringing in the replacements: Donor- and acceptor-substituted phenanthrenyl pairs as natural-base-pair replacements stabilize DNA duplexes and show interesting fluorescence behavior that varies depending on the substituent at the phenanthrene chromophore.

Catalysis

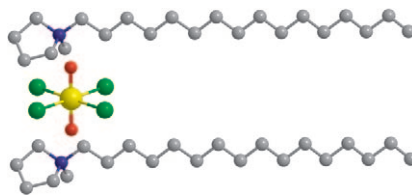
G. Christian, R. Stranger,*
B. F. Yates 646–655

A Comparison of N₂ Cleavage in Schrock's Mo[N₃N] and Laplaza–Cummins' Mo[N(R)Ar]₃ Systems



N₂ to ammonia: The differences in reactivity between Mo[*fac*-[RNCH₂CH₂]₃N], R = 3,5-(2,4,6-*i*Pr₃C₆H₂)₂C₆H₃, which is capable of converting N₂ to ammonia catalytically, and Mo[N(R)Ar]₃ (R = *t*Bu, Ar = 3,5-C₆H₃Me₂), which cannot, were explored by using density functional theory.

Rich smectic mesomorphism, including uncommon crystal smectic T phases, is exhibited by ionic liquid crystals based on *N*-alkyl-*N*-methylpyrrolidinium cations and various counteranions, including a new type of uranium-containing metallomesogens (e.g., see picture; C grey, Br green, N blue, O red, U yellow, H omitted). The U-containing mesogens are photoluminescent when dissolved in an ionic liquid, and the Eu^{III}-based liquid crystal shows intense red photoluminescence with high colour purity.



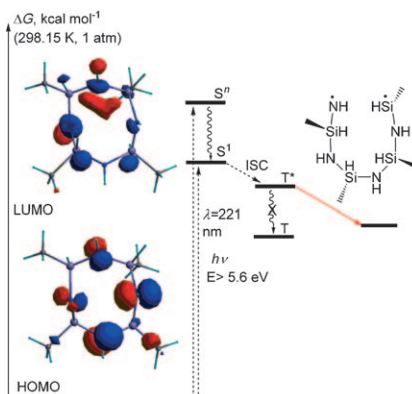
Liquid Crystals

*K. Goossens, K. Lava, P. Nockemann, K. Van Hecke, L. Van Meervelt, K. Driesen, C. Görrler-Walrand, K. Binnemans, T. Cardinaels** 656–674

Pyrrolidinium Ionic Liquid Crystals



Silicon networking: The vacuum-UV (VUV)-induced conversion of polyorganosilazanes into methyl-Si-O-Si networks was studied using 172, 185, and 222 nm UV light (see graphic). TOF-SIMS, XPS, and FTIR measurements as well as kinetic investigations were carried out to elucidate the occurring chemical reactions, such as Si–NH and Si–CH₃ degradation.



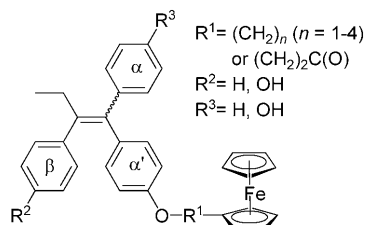
Surface Chemistry

L. Prager, L. Wennrich, R. Heller, W. Knolle, S. Naumov, A. Prager, D. Decker, H. Liebe, M. R. Buchmeiser** 675–683

Vacuum-UV Irradiation-Based Formation of Methyl-Si-O-Si Networks from Poly(1,1-Dimethylsilazane-co-1-methylsilazane)



Go bio! We report here the synthesis and cell-proliferation studies of the first derivatives of the breast cancer drug tamoxifen in which an organometallic moiety replaces the antiestrogenic side chain (see graphic). Structure–activity relationship studies show that the compound possessing two phenol groups and a carbonyl adjacent to the ferrocene has the best receptor-binding and cytotoxic properties.



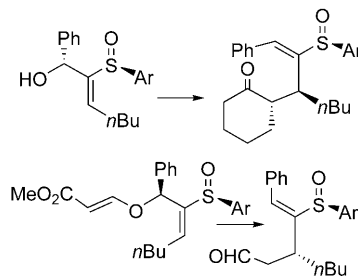
Bioorganometallics

A. Nguyen, S. Top, P. Pigeon, A. Vessières, E. A. Hillard, M.-A. Plamont, M. Huché, C. Rigamonti, G. Jaouen* 684–696

Synthesis and Structure–Activity Relationships of Ferrocenyl Tamoxifen Derivatives with Modified Side Chains



Consecutive construction: Diastereoselective Claisen rearrangements of allyl vinyl ethers with a sulfoxide at C-5 allow for the creation of up to two consecutive asymmetric centers and a new vinyl sulfoxide (see scheme).



Asymmetric Synthesis


R. Fernández de la Pradilla, C. Montero, M. Tortosa, A. Viso* 697–709

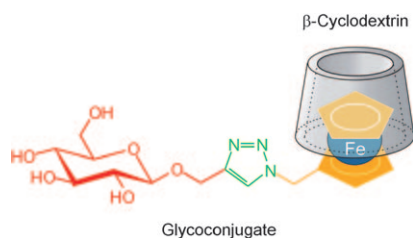
Asymmetric Claisen Rearrangements on Chiral Vinyl Sulfoxides



Molecular Sensors

J. M. Casas-Solvas, E. Ortiz-Salmerón,
J. J. Giménez-Martínez,
L. García-Fuentes,
L. F. Capitán-Vallvey,
F. Santoyo-González,*
A. Vargas-Berenguel* 710–725

 **Ferrocene–Carbohydrate Conjugates as Electrochemical Probes for Molecular Recognition Studies**

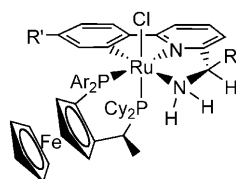


Glycoferrocenes as sensors: Ferrocene–carbohydrate conjugates with different tethers and sugars were synthesised by two convenient methods. The electrochemical behaviour of these compounds was investigated, as well as their complex formation with β -cyclodextrin (see figure) by NMR, ITC, CV and DPV experiments.

Asymmetric Hydrogenation

W. Baratta,* G. Chelucci, S. Magnolia,
K. Siega, P. Rigo 726–732


Highly Productive CNN Pincer Ruthenium Catalysts for the Asymmetric Reduction of Alkyl Aryl Ketones

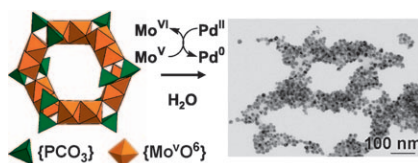


In a pinch: Chiral pincer complexes [RuCl(CNN)(Josiphos)] (see figure) are easily obtained by a one-pot reaction of [RuCl₂(PPh₃)₃] with 1-[1-(di-cyclohexylphosphano)ethyl]-2-(diarylphosphano)ferrocene (Josiphos) and racemic HCNN pincer ligands, promoted by acetic acid. These complexes are highly active and productive catalysts for the asymmetric hydrogenation and transfer hydrogenation of alkyl aryl ketones.

Nanoparticles

A. Dolbecq,* J.-D. Compain,
P. Mialane, J. Marrot, F. Sécheresse,
B. Keita, L. R. B. Holzle, F. Miserque,
L. Nadjo* 733–741


 **Hexa- and Dodecanuclear Polyoxomolybdate Cyclic Compounds: Application toward the Facile Synthesis of Nanoparticles and Film Electrodeposition**

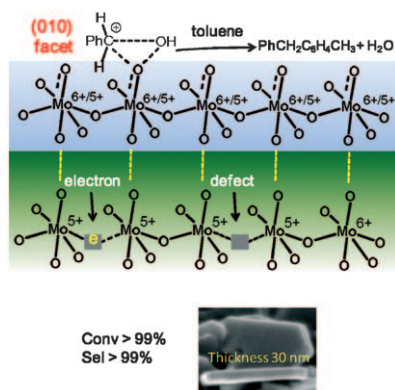


POMs to nanoPOMs: Two reduced polyoxometalates (POMs), one of which adopts a unique cyclohexane-like ring arrangement, are presented. The ring can be used as a precursor to POMs that incorporate organic ligands. Two applications of the redox properties of these species, namely, as reductants for the synthesis of Pd and Pt nanoparticles (see picture) and as precursors for the formation of films electrodeposited on glassy carbon are also shown.

Heterogeneous Catalysis

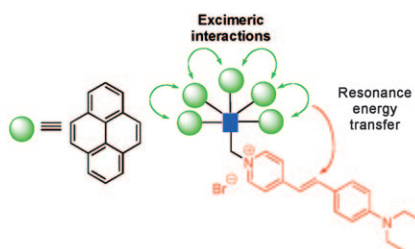
F. Wang,* W. Ueda* 742–753

 **High Catalytic Efficiency of Nanostructured Molybdenum Trioxide in the Benzylation of Arenes and an Investigation of the Reaction Mechanism**



On the face of it, the (010) facet of nanostructured MoO₃ is highly catalytically active and selective for the benzylation of various arenes with substituted benzyl alcohol. The reaction mechanism is discussed based on results from thermal, spectroscopic, and electronic techniques.

Molecular antennae: A series of dendrimeric compounds bearing pyrene units synthesized through the Huisgen reaction afford light-harvesting antennae based on the formation of intramolecular excimers (see picture). Three very efficient energy-transfer multi-emissive systems are obtained, one of which shows interesting, well-balanced emissions in deep-blue, blue-green, and red.



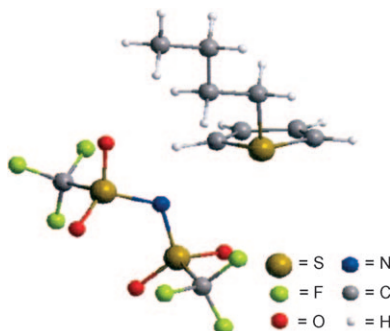
Energy Transfer

S. Cicchi,* P. Fabbrizzi, G. Ghini, A. Brandi, P. Foggi,* A. Marcelli, R. Righini, C. Botta* 754–764

Pyrene-Excimers-Based Antenna Systems



New electrolytes and lubricants: Cyclic sulfonium-based ionic liquids have been synthesized and characterized. Their physicochemical and electrochemical properties suggest their potential application as novel lubricants and electrolytes. The picture shows the structure of a representative cyclic sulfonium-based salt.

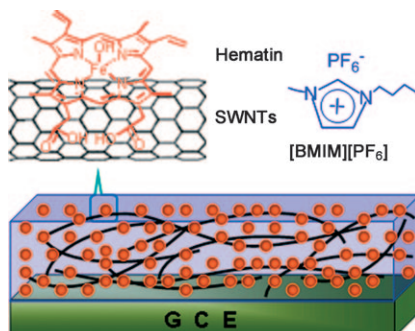


Ionic Liquids

Q. Zhang, S. Liu, Z. Li, J. Li, Z. Chen, R. Wang, L. Lu, Y. Deng* 765–778

Novel Cyclic Sulfonium-Based Ionic Liquids: Synthesis, Characterization, and Physicochemical Properties

A glassy carbon electrode (GCE) is modified with a composite of single-walled carbon nanotubes (SWNTs) and hematin, prepared in the ionic liquid 1-butyl-3-methylimidazolium hexafluorophosphate ([BMIM][PF₆]; see picture). Such functionalization accelerates electron transfer through a synergic effect, and the electrocatalytic activity toward trichloroacetic acid allows the construction of a biosensor.

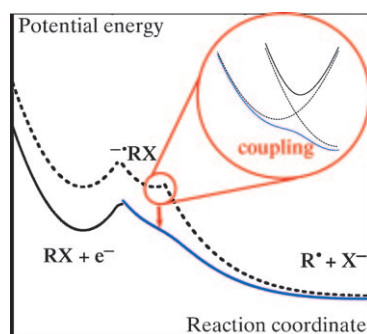


Porphyrin Nanoassembly

W. Tu, J. Lei,* H. Ju* 779–784

Functionalization of Carbon Nanotubes with Water-Insoluble Porphyrin in Ionic Liquid: Direct Electrochemistry and Highly Sensitive Amperometric Biosensing for Trichloroacetic Acid

A mechanism shift that depends on the position of the cyano group occurs in the reductive cleavage of the cyano-benzyl chloride (CBC) isomers in DMF. Whereas *m*-CBC is reduced along a two-step pathway (dotted curve), *o*- and *p*-CBC reduction follow a concerted pathway via a single transition state (full curve). The reason is that electronic coupling between the diabatic states of the products (magnified) eliminates the cleavage barrier for the *para* and *ortho* anion radicals. An intermediate anion radical only persists in the case of *m*-CBC.



Dissociative Electron Transfer


C. Costentin,* L. Donati, M. Robert* 785–792

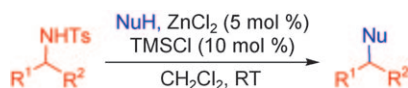
Passage from Stepwise to Concerted Dissociative Electron Transfer through Modulation of Electronic States Coupling



C–N Bond Cleavage


C.-R. Liu, M.-B. Li, C.-F. Yang,
S.-K. Tian* 793–797


 **Selective Benzylic and Allylic Alkylation of Protic Nucleophiles with Sulfonamides through Double Lewis Acid Catalyzed Cleavage of sp^3 Carbon–Nitrogen Bonds**




Cutting deep into C–N bonds: A highly efficient benzylic and allylic alkylation of protic carbon and sulfur nucleophiles with sulfonamides has been developed through $ZnCl_2$ -TMSCl-catalyzed cleavage of sp^3 C–N bonds at room temperature (see scheme).

* Author to whom correspondence should be addressed

 Supporting information on the WWW (see article for access details).

 Full Papers labeled with this symbol have been judged by two referees as being “very important papers”.

 A video clip is available as Supporting Information on the WWW (see article for access details).

SERVICE

Spotlights 564 Authors 800 Keywords 801 Preview 803

Issue 2/2008 was published online on December 23, 2008